

# Exploring the role of the phage-specific insert of bacteriophage $\Phi$ 11 dUTPase

Kinga Nyíri<sup>1,2</sup> · Veronika Papp-Kádár<sup>1,2</sup> · Judit E. Szabó<sup>1,2</sup> ·  
Veronika Németh<sup>1</sup> · Beáta G. Vértessy<sup>1,2</sup>

Received: 23 July 2015 / Accepted: 27 July 2015  
© Springer Science+Business Media New York 2015

**Abstract** dUTPases are essential for maintaining genome integrity. Recently, in the case of a dUTPase from a *Staphylococcal* phage, another different physiological function was also suggested. Namely, it was shown that dUTPase from the *Staphylococcus aureus* bacteriophage  $\Phi$ 11 is capable of binding to the *Staphylococcal* Stl repressor protein. This binding interferes with the function of Stl. In the present study, we investigated the putative role of a phage dUTPase-specific peptide segment in the interaction of dUTPase with Stl and in impeding Stl–DNA complex formation. We show that dUTPase from *Mycobacterium tuberculosis* that lacks the phage-specific insert is also capable of disrupting the complexation between Stl and DNA. Hence, the insert segment is not essential for perturbation of the Stl function. However, we also demonstrate that in case of the phage dUTPase, the insert-lacking construct is deficient in perturbation of Stl activity. These findings clearly indicate that the phage-specific insert has a well-defined role only in the context of the phage dUTPase.

**Keywords** dUTPase · Non-canonical insert · Protein–protein interaction · Protein–DNA interaction · *Staphylococcal* repressor

## Introduction

Genome integrity is essential in all living organisms. Numerous cellular pathways are involved in maintaining the integrity of genomic DNA, among which both sanitization of nucleotide pools and proper recognition and repair of damage sites are highly important. The enzyme family of dUTPases is responsible for maintaining the ample supply of nucleotides by decreasing the dUTP concentration in the cellular milieu [1, 2]. The product of the dUTPase enzymatic reaction is dUMP, which also serves as the precursor for dTTP biosynthesis. Knockout or silencing the *dut* gene encoding dUTPases leads to lethal cellular consequences in various species [3–9]. From the structural viewpoint, there are two major dUTPase enzyme families:  $\beta$ -pleated trimers and  $\alpha$ -helical dimers [2, 10, 11]. Most dUTPases belong to the  $\beta$ -pleated trimer family, including also several representatives from viruses and bacteriophages [12–19].

In addition to the well-conserved dUTPase fold and the five conserved sequence motifs within the trimeric dUTPase family, several dUTPases also possess species-specific additional segments (Fig. 1a). It has been shown that the amino-terminal extension of eukaryotic dUTPases functions as a localization signal [20–25]; this motif of rat dUTPase was also suggested to have crucial role in forming interaction with the transcriptional factor PPAR $\alpha$  [26]. Besides the N-terminal extension, both isoforms of the *Drosophila melanogaster* dUTPase contain a 28-residue-long segment at the C-terminus that is found only in the

---

This study is dedicated to Magdolna Hargittai on her 70th birthday to celebrate her discoveries in the field of molecular symmetry, a key issue from chemistry to biology.

---

✉ Kinga Nyíri  
nyiri.kinga@ttk.mta.hu

✉ Beáta G. Vértessy  
vertessy@kutatok.org

<sup>1</sup> Institute of Enzymology, RCNS, Hungarian Academy of Sciences, Budapest2 Magyar tudósok körútja, 1117, Hungary

<sup>2</sup> Department Biotechnology, Budapest University of Technology and Economics, Budapest4 Szent Gellért tér, 1111, Hungary

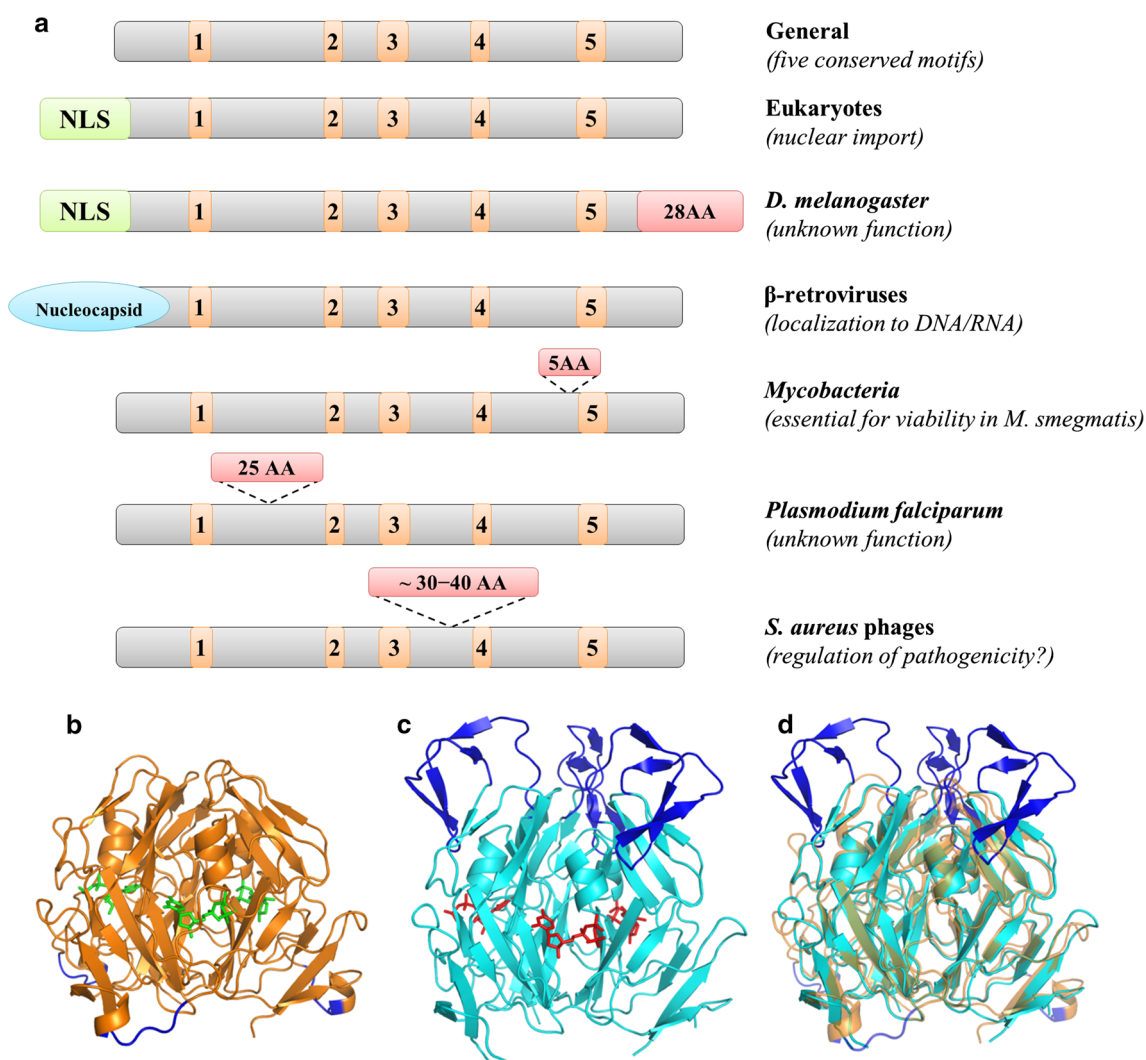


**Fig. 1** Non-canonical segments of dUTPases. **a** Schematic representation of the non-canonical segments of dUTPases and their function, **b** X-ray crystal structure of the *Mycobacterium tuberculosis* dUTPase (mtDUT, PDB ID: 2PY4), protein trimer is shown in *cartoon representation*, substrate analogs (dUPNPP) as *sticks*. The *Mycobacteria*-specific insert colored *dark blue* other residues *orange*, ligands *green*. **c** X-ray crystal structure of the  $\Phi$ 11 bacteriophage dUTPase

( $\Phi$ 11DUT<sup>WT</sup>, PDB ID: 4GV8), protein trimer is shown in *cartoon representation*, substrate analogs (dUPNPP) as *sticks*. The phage-specific insert colored *dark blue* other residues *cyan*, ligands *red*. **d** Superimposition of the mtDUT and  $\Phi$ 11DUT<sup>WT</sup> structures. Coloring and representation are according to (b) and (c); ligands are not shown. The phage-specific insert did not affect the core dUTPase fold (Color figure online)

*Drosophila* dUTPases, and showed no significant effect on the enzyme activity *in vitro*; however, it might modulate enzyme function *in vivo* [21, 27, 28]. In  $\beta$ -retroviral dUTPases, an amino-terminal extension is constituted by the retroviral nucleocapsid protein, which is hypothesized to localize dUTPase to the DNA/RNA, thereby enhancing the fidelity of replication by *in situ* lowering the dUTP level at the site of reverse transcription [15, 29, 30].

In *Mycobacterial* dUTPase enzymes, a small insert of five residues has been shown to be dispensable for enzymatic activity, but essential for some yet undiscovered cellular activity (Fig. 1b) [31]. The function of the 25-residue-long insert situated between the second and

third conserved motifs in *Plasmodium falciparum* dUTPase has not yet been identified either [32].

In a recently discovered dUTPase protein, another moonlighting function was suggested, namely involvement in regulation of horizontal gene transfer in *Staphylococcus aureus* [33]. In this instance, the dUTPase enzyme from the *S. aureus* phage  $\Phi$ 11 was shown to possess derepression activity via removal of the master repressor StI protein from its cognate DNA site, thereby ensuring replication of a *S. aureus* pathogenicity island (SaPI<sub>bov1</sub>) genetic element. We have shown that the derepression by  $\Phi$ 11 dUTPase is only possible if dUTP is cleared from the nucleotide pool. This may indicate that dUTPase-mediated activation of the

SaPI<sub>bov1</sub> promotes the genomic stability of this mobile genetic element [34].

Interestingly, compared to other dUTPases, the *S. aureus* phage  $\Phi$ 11 dUTPase ( $\Phi$ 11DUT<sup>WT</sup>) possesses a phage-specific insert of 26 residues situated between the third and fourth conserved motifs (cf. Fig. 1c) [18]. This feature of a ca. 30–40-residue-long inserted segment is well observed also in other *Staphylococcus* phage dUTPases; however, to our knowledge, no other dUTPase possesses such segments at this location. It has been suggested that the insert has a crucial role in StI-mediated SaPI replication and dUTPase activity, based on a deletion of a 39-residue-long region from  $\Phi$ 11 dUTPase, containing the insert ( $\Phi$ 11DUT <sup>$\Delta$ 96A–134L</sup>) [33]. Sequence alignment of the  $\Phi$ 11 dUTPase with other dUTPases revealed that this deletion included residues from the fourth catalytic motif of the dUTPase, which explains the loss of enzymatic activity. The 3D crystal structure obtained by our group also affirmed the importance of these residues in formation of the active site [18]. This compromises the hypothesis based on the studies of the  $\Phi$ 11DUT <sup>$\Delta$ 96A–134L</sup> mutant. Based on the structure of  $\Phi$ 11DUT<sup>WT</sup>, we found no interaction of the 26-residue-long phage-specific insert with the active site. This motif also did not cause any detectable major interference with the folding of the dUTPase trimer [18]. This led us to the hypothesis that the insert does not influence the dUTPase activity, which contradicts the former model. To verify this suggestion, we constructed a mutant  $\Phi$ 11 dUTPase, in which the conserved motifs are still intact, while most part of the insert (20 residues out of the 26) is removed ( $\Phi$ 11DUT <sup>$\Delta$ 101G–122Q</sup>) [18]. This  $\Phi$ 11DUT <sup>$\Delta$ 101G–122Q</sup> protein showed the same activity as the wild-type  $\Phi$ 11 dUTPase. We also studied the role of the insert in dUTPase enzymatic activity using the  $\Phi$ 11DUT<sup>F108W</sup> mutant in which we introduced a tryptophan fluorophore into the phage-specific insert [35–37]. There were no observable fluorescence spectral changes upon binding of either nucleotide ligand to this protein that possessed the same enzymatic properties as  $\Phi$ 11DUT<sup>WT</sup> [18]. This further supported our hypothesis that the phage-specific insert has no effect on dUTPase activity of the  $\Phi$ 11 dUTPase. However, the role of the phage-specific insert in StI-binding and derepression activity has not yet been well characterized.

In an attempt to deal with this intriguing open question, in the present study we aimed to explore the role of the phage-specific insert in the interaction with StI and in the disruption of StI–DNA complex. We show that StI is fully capable of binding to and inhibiting an insert-lacking mutant construct of phage dUTPase, with practically the same characteristics that also govern StI binding and inhibition to wild-type phage dUTPase. Our data also

show, however, that the insert-lacking mutant construct of dUTPase is deficient in derepression activity. Though in another protein context, namely in the case of *Mycobacterium tuberculosis* dUTPase, which also lacks the phage-specific insert, we find strong derepression activity for StI. This shows on the one hand that derepression of StI may be observed in a cross-species setting and on the other hand that the phage-specific insert has a distinct role only within the protein structure context of the phage dUTPase.

## Methods

### Cloning and expression of proteins

The cloning of cDNA of StI protein into pGEX-4T-1 and  $\Phi$ 11 dUTPase into pETDuet-1 vectors and the deletion of the insert by site-directed mutagenesis to obtain  $\Phi$ 11DUT <sup>$\Delta$ 101G–122Q</sup> are described in our previous works [18, 34, 38]. Cloning of the recombinant *Mycobacterium smegmatis* dUTPase (mtDUT) carrying an N-terminal hexa-His tag to pET19-b vector was published in an earlier work [39].

Vectors coding StI and  $\Phi$ 11 dUTPases were transformed into *Escherichia coli* strain BL21 Rosetta (DE3) and propagated in 500 ml Luria-Bertani medium on 310 K till OD<sub>600</sub> = 0.6, and then the culture was induced with 0.5 mM isopropyl- $\beta$ -D-thiogalactoside (IPTG). After induction, the cell cultures were grown at 303 K for further 4 h. Finally the cells were harvested by centrifugation and stored at 193 K. The mtDUT protein was expressed in *E. coli* BL21(DE3) pLysS cells following the procedure described above; however, after induction by IPTG, cells were tempered on 310 K for 3 h.

### Purification of proteins

For purification of StI, cell pellets containing glutathione S-transferase–StI (GST–StI) fusion protein were solubilized using Potter–Elvehjem homogenizer in 20 ml buffer A (15 ml HEPES (pH 7.5), 200 mM NaCl) supplemented with 2 mM dithiothreitol (DTT), 1 % Triton X-100, ca. 2  $\mu$ g/ml RNase and DNase and one tablet of Complete ULTRA Tablets, Mini EDTA-free protease inhibitor. Cell suspensions were sonicated (4  $\times$  1 min) and centrifuged (16,000g for 30 min). The resulting supernatant was loaded on a pre-equilibrated benchtop glutathione-agarose affinity-chromatography column (GE Healthcare). The column was washed with ten volumes of buffer A, and then on-column cleavage for the removal of the GST-tag was performed by addition of 80 cleavage units of thrombin (GE Healthcare). Following the overnight cleavage, the purified protein was obtained in the flow-through fraction. Purification of  $\Phi$ 11

dUTPases was performed as described previously [38]; briefly supernatant resulting from centrifugation of cell lysate was purified on Q-Sepharose (GE Healthcare) anion-exchange column, followed by gel filtration on a Superdex 75 column (GE Healthcare) using an AKTA Explorer purifier. Protein purification of mtDUT was carried out based on our previously published protocol [40]. The final supernatant after cell extraction was loaded on a NiNTA column (Novagen), and the first salt wash was followed by washing with 50 mM Tris-HCl, pH 7.5, buffer containing 30 mM NaCl, and 50 mM imidazole. Elution of the mtDUT was performed with 0.5 M imidazole solution (pH 7.5), and the protein was afterward dialyzed into 10 mM Tris-HCl (pH 7.0) buffer supplemented with 50 mM NaCl, 10 mM MgCl<sub>2</sub>, and 0.1 mM TCEP.

All protein preparations were used freshly or were flash-frozen in liquid nitrogen and stored at 193 K and were proven to be >95 % pure as judged by SDS-PAGE.

### Protein quantification

NanoDrop 2000 UV-Vis spectrophotometer was used for measuring protein concentration using the following  $A^{0.1\%}_{280}$  values 1.087, 0.786, 0.810, and 0.166 ml mg<sup>-1</sup>\*cm<sup>-1</sup> for StI,  $\Phi11DUT^{WT}$ ,  $\Phi11DUT^{\Delta101G-122Q}$ , and mtDUT, respectively, calculated based on amino acid composition [41] (<http://web.expasy.org/protparam/>).

### Native polyacrylamide gel electrophoresis (native PAGE)

Native gel electrophoresis was performed in 12 % polyacrylamide gel. After pre-electrophoresis with constant voltages of 100 V for 1 h, 20  $\mu$ l aliquots of the premixed samples was applied on the gel. Electrophoresis was performed for 3.5 h on 150 V in pH 8.7 in electrophoresis buffer, containing 2.5 mM Tris base, and 19.2 mM glycine. Denaturation during the electrophoresis caused by the evolving heat was avoided by cooling the tank on ice. Coomassie Brilliant Blue dye was used to stain the gels.

### Steady-state kinetics

Proton release during the transformation of dUTP into dUMP and PPi was followed at 559 nm and 293 K using a Jasco V550 spectrophotometer [15]. Reaction mixtures contained 50 nM dUTPase enzyme in 1 mM HEPES-HCl (pH 7.5) supplemented with 5 mM MgCl<sub>2</sub>, 150 mM KCl, and 40  $\mu$ M phenol red pH indicator. The reaction was started with the addition of 30 mM dUTP after pre-incubation of the two proteins for 5 min. All measurements at different StI concentrations were repeated three times. The

initial velocities were determined from the slope of the first 10 % of the progress curves. Quadratic binding equation was fitted to the data.

### Electrophoretic mobility shift assay (EMSA)

A 57-mer dsDNA oligonucleotide (5'-GCTCATATTATT CCTCTCCTACCATTTTATCTCTAATTGAGATATTTA TATTCAGAT-3') was used in electrophoretic mobility shift assay (EMSA) experiments. Complementary oligonucleotides were custom-synthesized by Eurofins MWG Operon and hybridized by controlled gradual cooling after 5-min incubation on 95 °C. Proteins were mixed with 100 ng DNA in 20  $\mu$ l total volume, and concentration of NaCl was set to 100 mM in each mixture. Samples were loaded onto 12 % polyacrylamide gel following 15-min incubation at 4 °C. After 1 h pre-electrophoresis of the gel in TBE buffer (89 mM Tris base 89 mM boric acid and 2 mM EDTA, pH 8.3), electrophoresis was performed for 70 min at room temperature. Bands were detected after staining with GelRed (Biotium), using a Uvi-Tec gel documentation system (Clever Scientific Ltd., Rugby, UK).

### Results and discussion

Our previous studies showed that the StI-dUTPase interaction can be well characterized by native polyacrylamide gel electrophoresis, and complex formation could be made clearly visible with this method [34, 42]. Besides StI is proven to be an effective dUTPase inhibitor; thus, enzyme inhibition curves provide information on the binding characteristics of StI to dUTPases [34, 42]. In this study, the role of the phage-specific insert of the  $\Phi11$  dUTPase in forming interactions with StI was investigated using these two different methods. First, the wild-type and the truncated  $\Phi11$  dUTPase proteins and their mixtures with StI were run on native polyacrylamide gel. Based on the native gel electrophoresis results, the truncated protein shows very similar complexation pattern with StI as compared to the wild type (Fig. 2a). At 1:1 monomer ratio, the formed complex clearly appears at a distinct upper position as compared to StI and dUTPase bands (Complex A, Fig. 2a). Decreasing the amount of StI in the protein mixtures results in the appearance of the excess dUTPase and a band of a second complex type (Complex B, Fig. 2a). Although the band of Complex B appears close to the StI band, since  $\Phi11DUT$  was in excess that is certainly not free StI. The two types of complexes have different stoichiometries. Based on the applied concentrations, the StI/ $\Phi11DUT$  ratio is higher in Complex A as compared to that in Complex B. Previous electrospray ionization native mass spectrometry measurements of the mixture of StI and  $\Phi11DUT^{WT}$

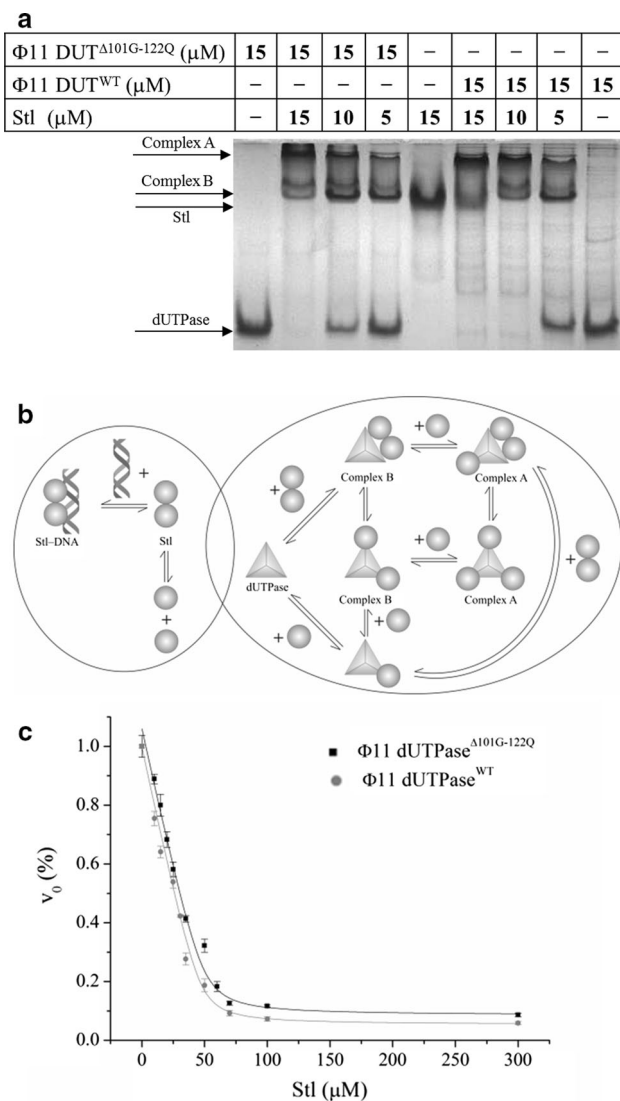


**Fig. 2** Stl-binding ability of  $\Phi 11$ dUTPase $^{\Delta 101G-122Q}$ . **a** Native gel electrophoresis experiment was performed to investigate the Stl-binding ability of  $\Phi 11$ dUTPase $^{\Delta 101G-122Q}$  comparing to  $\Phi 11$ dUTPase<sup>WT</sup>. Species and concentrations given in monomers are indicated. The mixtures of Stl and dUTPases show up a band in distinct position comparing to the individual proteins, which clearly indicates the complex formation.  $\Phi 11$ dUTPase $^{\Delta 101G-122Q}$  shows very similar complexation pattern to  $\Phi 11$ dUTPase<sup>WT</sup>. **b** Schematic view of the possible complex equilibria between Stl (*sphere*), dUTPases (*triangle*), and DNA (*helices*). This model may offer explanations for the observed experimental results. The dimerization of Stl and the formation of Complex B were proven by our previous electrospray ionization native mass spectrometry measurements [34]. The existence of Complex A is shown by native polyacrylamide gel electrophoresis. We suggest that as the general prophage regulator repressors, Stl also binds DNA as a dimer. We applied this simple model; however, some more complex patterns may possibly exist. **c** Activity of the  $\Phi 11$  dUTPase $^{\Delta 101G-122Q}$  and  $\Phi 11$ dUTPase<sup>WT</sup> was measured in the presence and absence of Stl. Each measurement was repeated three times. The quadratic binding equation was fit to the data resulted in the apparent  $K_i = 1.2 \pm 0.8$  nM for dUTPase<sup>WT</sup> and  $K_i = 1.5 \pm 0.6$  nM for dUTPase $^{\Delta 101G-122Q}$ . The total change in amplitude of the activity was >90 % for both proteins

revealed that one of the complexes results from the interaction of a trimer  $\Phi 11$ dUTPase<sup>WT</sup> with an Stl dimer or with two Stl monomers ( $\Phi 11$ dUTPase<sub>3</sub>Stl<sub>2</sub>) [34]. Considering the relative intensity of the bands of the complex and the free proteins at 3:1 dUTPase/Stl monomer ratios, we hypothesize that Complex B reflects the  $\Phi 11$ dUTPase<sub>3</sub>Stl<sub>2</sub> stoichiometry, and consequently, Complex A has the stoichiometry of  $\Phi 11$ dUTPase<sub>3</sub>Stl<sub>3</sub> [34].

Considering the potential complexation equilibria in the three component systems, Fig. 2b summarizes some major possibilities that may offer explanations to our observed experimental results and serves as a model for designing further studies. Our previous electrospray ionization native mass spectrometry results revealed that Stl exists as monomer and dimer in solution [34]. The experimentally observed Stl- $\Phi 11$ dUTPase<sup>WT</sup> complex did not provide any indication of dissociation of the dUTPase trimer [34], which is also in agreement with the general consideration that the trimeric dUTPases are extremely stable in this oligomer form in solution [35]. Thus, the monomer-trimer equilibrium was excluded from this model. Our experimental data support that two types of complexes present between Stl and  $\Phi 11$  dUTPase (Complexes A and B, Fig. 2a), but the exact molecular architecture of those is yet unknown; hence, two possible representations of these complexes are shown in Fig. 2b.

Since the two dUTPases showed similar patterns of the bands, thus we suggest that the same statements are also valid for the truncated  $\Phi 11$ dUTPase $^{\Delta 101G-122Q}$  protein. Nevertheless, there is a slight difference in the distribution of the proteins between the two types of complexes at the same dUTPase/Stl ratios.

It has been shown that the truncated  $\Phi 11$ dUTPase $^{\Delta 101G-122Q}$  has similar dUTPase activity as compared to that of  $\Phi 11$ dUTPase<sup>WT</sup> and that Stl effectively inhibits the  $\Phi 11$ dUTPase<sup>WT</sup> enzyme [18, 34]. Therefore, we also investigated the interaction of Stl with  $\Phi 11$ dUTPase $^{\Delta 101G-122Q}$  by enzyme activity measurements applying varying Stl concentrations in this work (Fig. 2c). The activity of  $\Phi 11$ dUTPase<sup>WT</sup> and  $\Phi 11$ dUTPase $^{\Delta 101G-122Q}$  was measured to be  $7.3 \pm 0.1$  s<sup>-1</sup> and  $7.6 \pm 0.3$  s<sup>-1</sup>. The maximal activity decrease was found to be  $6.9 \pm 0.1$  s<sup>-1</sup> for  $\Phi 11$ dUTPase<sup>WT</sup> and  $7.4 \pm 0.3$  s<sup>-1</sup> for  $\Phi 11$ dUTPase $^{\Delta 101G-122Q}$ , which is equal to  $94 \pm 2$  % and  $98 \pm 4$  % inhibitions for the two dUTPases, respectively. We observed very similar inhibition curves for the two dUTPases, with the apparent equilibrium constants of  $K_i = 1.2 \pm 0.8$  nM for  $\Phi 11$ dUTPase<sup>WT</sup> and  $K_i = 1.5 \pm 0.6$  nM for  $\Phi 11$ dUTPase $^{\Delta 101G-122Q}$  (Fig. 2c).

All in all, we concluded that the insert has no specific role in Stl binding. This conclusion was also supported by our study on the interaction between Stl and *M. tuberculosis* dUTPase (mtDUT), which does not contain the

phage-specific insert [42]. Previously we observed complex formation between Stl and mtDUT on native gel, and based on enzyme activity measurements, the inhibitory effect of Stl can also be described with a very low apparent inhibitory constant,  $K_i = 6.8 \pm 4.4$  nM, and the overall inhibition was found to be  $81 \pm 10$  % [42]. We also found elevated cellular dUTP levels and disturbed colony formation upon expressing Stl protein in *M. smegmatis*. These alterations are undoubtedly due to the inhibition of the bacterial dUTPase by Stl. Altogether strong interaction between Stl and *Mycobacterial* dUTPases was proven to exist by in vitro and in vivo experiments [42].

Having established that the phage-specific insert has no observable effect on the complex formation between Stl and dUTPases, we tested whether this insert may have any role in perturbation of the Stl function.

As a life-cycle-regulating repressor, Stl binds to specific DNA segments and herewith prevents the replication and excision of the SaPI mobile genetic element. We hypothesize that as it is well known for other prophage repressors, Stl binds DNA as a dimer (Fig. 2b). Although since Stl regulates the expression of at least three proteins higher-order complexes between Stl and DNA may also possibly exist [43], further investigations are needed to address this question.

It has been shown by in vitro experiments that the DNA binding of Stl repressor is disturbed by  $\Phi 11\text{DUT}^{\text{WT}}$  [33, 34]. In these studies, the DNA binding of Stl was observed by the change in electrophoretic mobility of a DNA oligo upon protein binding: The DNA band appears at a higher position when bound to Stl protein as compared to the position of free DNA. So the complex equilibria were shifted toward the free DNA form upon addition of  $\Phi 11\text{DUT}^{\text{WT}}$  to the DNA–Stl mixture (Fig. 2b). It has also been presented that the Stl– $\Phi 11\text{DUT}^{\text{WT}}$  interaction results in derepression and SaPI replication in *S. aureus* [33]. Thus, the in vivo derepression activity of  $\Phi 11\text{DUT}^{\text{WT}}$  was proven to be well described by the applied in vitro experimental method.

The role of the insert in disturbing the DNA-binding ability of Stl was tested with electrophoretic mobility shift assay experiments (Fig. 3a). If  $\Phi 11\text{DUT}^{\text{WT}}$  was added to the DNA–Stl mixture, the resulting band appears at the same position as the free DNA, confirming the derepression activity of the phage protein (Fig. 3a) [33, 34]. However, in case of adding  $\Phi 11\text{DUT}^{\Delta 101\text{G}-122\text{Q}}$  to the same Stl–DNA mixture, the band shows up at the position of the Stl–DNA complex. This result suggests that the insert is necessary for the disruption of the Stl–DNA complex and so the derepression activity of  $\Phi 11$  dUTPase. We also tested the derepression ability of the mtDUT, which lacks the phage-specific insert, with the same method (Fig. 3b). The *M. tuberculosis* dUTPase showed similar derepression activity in EMSA experiments as the

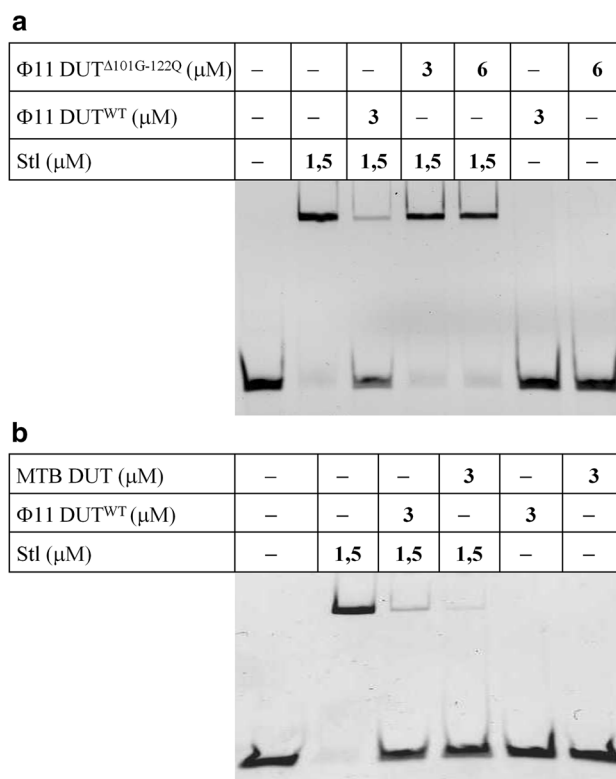


**Fig. 3** Derepression activity of  $\Phi 11\text{DUT}^{\Delta 101\text{G}-122\text{Q}}$  and mtDUT. Electrophoretic mobility shift assay experiments were performed to investigate the derepression activity of  $\Phi 11\text{DUT}^{\Delta 101\text{G}-122\text{Q}}$  and mtDUT. Species and concentrations given in monomers are indicated in the figure. **a** Lack of derepression was observed in the case of  $\Phi 11\text{DUT}^{\Delta 101\text{G}-122\text{Q}}$  even at elevated concentration of the protein. **b** Unless mtDUT lacks the phage-specific insert, it has similar derepression activity comparing to  $\Phi 11\text{DUT}^{\text{WT}}$

$\Phi 11\text{DUT}^{\text{WT}}$  protein (Fig. 3b). This result led us to the conclusion that the insert is only necessary for perturbing Stl–DNA interaction in the context of  $\Phi 11$  dUTPase.

Considering that the truncated  $\Phi 11$  dUTPase has very similar overall apparent  $K_i$  as compared to the wild-type protein, the change in its derepression activity can only be explained with more complex or non-equilibrium models.

## Conclusions

Besides the well-conserved protein structural core, several trimeric dUTPases contain non-canonical segments that may be related to moonlighting functions of these enzymes. In this work, we explored the role of the phage-specific insert of the  $\Phi 11$  bacteriophage dUTPase, which acts as a derepressor of a *S. aureus* pathogenicity island (SaPI<sub>bov1</sub>) through interacting with Stl, the master repressor of this mobile genetic element. We have shown previously with the truncated enzyme mutant  $\Phi 11\text{DUT}^{\Delta 101\text{G}-122\text{Q}}$  that this extra segment does not influence dUTPase activity [18]. In

this study, we addressed the role of the phage-specific insert in protein–protein interaction and derepression. The insert was found dispensable in complex formation with StI based on native gel electrophoresis experiments. The truncated mutant  $\Phi 11\text{DUT}^{\Delta 101\text{G}-122\text{Q}}$  showed also very similar inhibition characteristics as compared to the wild-type protein,  $\Phi 11\text{DUT}^{\text{WT}}$ . It has been proven by electrophoretic mobility shift assay (EMSA) tests that  $\Phi 11\text{DUT}^{\text{WT}}$  effectively disrupts the StI–DNA complex [33, 34]. On the contrary, EMSA experiments indicated that  $\Phi 11\text{DUT}^{\Delta 101\text{G}-122\text{Q}}$  does not interfere with the interaction between StI and DNA. This led us to a conclusion that within its own protein context the phage-specific insert is essential. To provide a more general view on this subject, we tested whether *M. tuberculosis* dUTPase is able to disturb the StI–DNA complex formation in vitro. Our results suggest cross-species existence of the derepression ability of dUTPases and allowing the design in vivo experiments to further investigate this molecular switch.

**Acknowledgments** Authors thank for the support of Hungarian Scientific Research Fund OTKA [NK 84008, K109486]; Baross Program of the New Hungary Development Plan [3DSTRUCT, OMF-00266/2010 REG-KM-09-1-2009-0050]; Hungarian Academy of Sciences ([TTK IF-28/2012]; MedinProt program); the ICGEB Research Grant to BGV; and the European Commission FP7 Biostruct-X project [Contract No. 283570]. Funding for open access charge: Hungarian Academy of Sciences.

## References

- Vértessy BG, Tóth J (2009) Keeping uracil out of DNA: physiological role, structure and catalytic mechanism of dUTPases. *Acc Chem Res* 42:97–106
- Persson R, Cedergren-Zeppezauer ES, Wilson KS (2001) Homotrimeric dUTPases; structural solutions for specific recognition and hydrolysis of dUTP. *Curr Protein Pept Sci* 2:287–300
- Taylor AF, Weiss B (1982) Role of exonuclease III in the base excision repair of uracil-containing DNA. *J Bacteriol* 151:351–357
- el-Hajj HH, Zhang H, Weiss B (1988) Lethality of a dut (deoxyuridine triphosphatase) mutation in *Escherichia coli*. *J Bacteriol* 170:1069–1075
- Dengg M, Garcia-Muse T, Gill SG et al (2006) Abrogation of the CLK-2 checkpoint leads to tolerance to base-excision repair intermediates. *EMBO Rep* 7:1046–1051
- Siaud N, Dubois E, Massot S et al (2010) The SOS screen in *Arabidopsis*: a search for functions involved in DNA metabolism. *DNA Repair (Amst)* 9:567–578
- Dubois E, Córdoba-Cañero D, Massot S et al (2011) Homologous recombination is stimulated by a decrease in dUTPase in *Arabidopsis*. *PLoS ONE* 6:e18658
- Castillo-Acosta VM, Aguilar-Pereyra F, García-Caballero D et al (2013) Pyrimidine requirements in deoxyuridine triphosphate nucleotidohydrolase deficient *Trypanosoma brucei* mutants. *Mol Biochem Parasitol* 187:9–13
- Muha V, Horváth A, Békési A et al (2012) Uracil-containing DNA in *Drosophila*: stability, stage-specific accumulation, and developmental involvement. *PLoS Genet* 8:e1002738
- Nagy GN, Leveles I, Vértessy BG (2014) Preventive DNA repair by sanitizing the cellular (deoxy)nucleoside triphosphate pool. *FEBS J* 281:4207–4223
- Hemsworth GR, González-Pacanoska D, Wilson KS (2013) On the catalytic mechanism of dimeric dUTPases. *Biochem J* 456:81–88
- Prasad GS, Stura EA, Mcrec DE et al (1996) Crystal structure of dUTP pyrophosphatase from feline immunodeficiency virus. *Protein Sci* 5:2429–2437
- Dauter Z, Persson R, Rosengren AM et al (1999) Crystal structure of dUTPase from *Equine Infectious Anaemia Virus*; active site metal binding in a substrate analogue complex. *J Mol Biol* 285:655–673
- Samal A, Schormann N, Cook WJ et al (2007) Structures of vaccinia virus dUTPase and its nucleotide complexes. *Acta Crystallogr D Biol Crystallogr* 63:571–580
- Németh-Pongrácz V, Barabás O, Fuxreiter M et al (2007) Flexible segments modulate co-folding of dUTPase and nucleocapsid proteins. *Nucleic Acids Res* 35:495–505
- Takács E, Barabás O, Petoukhov MV et al (2009) Molecular shape and prominent role of beta-strand swapping in organization of dUTPase oligomers. *FEBS Lett* 583:865–871
- Badalucco L, Poudel I, Yamanishi M et al (2011) Crystallization of *Chlorella* deoxyuridine triphosphatase. *Acta Crystallogr Sect F Struct Biol Cryst Commun* 67:1599–1602
- Leveles I, Németh V, Szabó JE et al (2013) Structure and enzymatic mechanism of a moonlighting dUTPase. *Acta Crystallogr D Biol Crystallogr* 69:2298–2308
- Tormo-Más MÁ, Donderis J, García-Caballer M et al (2013) Phage dUTPases control transfer of virulence genes by a proto-oncogenic G protein-like mechanism. *Mol Cell* 49:947–958
- Tinkelenberg B, Fazzone W, Lynch FJ, Ladner RD (2003) Identification of sequence determinants of human nuclear dUTPase isoform localization. *Exp Cell Res* 287:39–46
- Békési A, Zagyva I, Hunyadi-Gulyás E et al (2004) Developmental regulation of dUTPase in *Drosophila melanogaster*. *J Biol Chem* 279:22362–22370
- Muha V, Zagyva I, Venkei Z et al (2009) Nuclear localization signal-dependent and -independent movements of *Drosophila melanogaster* dUTPase isoforms during nuclear cleavage. *Biochem Biophys Res Commun* 381:271–275
- Merényi G, Kónya E, Vértessy BG (2010) *Drosophila* proteins involved in metabolism of uracil–DNA possess different types of nuclear localization signals. *FEBS J* 277:2142–2156
- Róna G, Marfori M, Borsos M et al (2013) Phosphorylation adjacent to the nuclear localization signal of human dUTPase abolishes nuclear import: structural and mechanistic insights. *Acta Crystallogr D Biol Crystallogr* 69:2495–2505
- Róna G, Pálkás HL, Borsos M et al (2014) NLS copy-number variation governs efficiency of nuclear import—case study on dUTPases. *FEBS J* 281:5463–5478
- Chu R, Lin Y, Rao MS, Reddy JK (1996) Cloning and identification of rat Deoxyuridine Triphosphatase as an inhibitor of peroxisome proliferator-activated receptor alpha. *J Biol Chem* 271:27670–27676
- Fiser A, Vértessy BG (2000) Altered subunit communication in subfamilies of trimeric dUTPases. *Biochem Biophys Res Commun* 279:534–542
- Kovári J, Barabás O, Takács E et al (2004) Altered active site flexibility and a structural metal-binding site in eukaryotic dUTPase: kinetic characterization, folding, and crystallographic studies of the homotrimeric *Drosophila* enzyme. *J Biol Chem* 279:17932–17944
- Bergman A-C, Björnberg O, Nord J et al (1994) The protein p30, encoded at the gag-pro junction of *Mouse Mammary Tumor*

- Virus*, is a dUTPase fused with a nucleocapsid protein. *Virology* 204:420–421
30. Barabás O, Rumlová M, Erdei A et al (2003) dUTPase and nucleocapsid polypeptides of the *Mason-Pfizer Monkey Virus* form a fusion protein in the virion with homotrimeric organization and low catalytic efficiency. *J Biol Chem* 278:38803–38812
  31. Pecsí I, Hirmondo R, Brown AC et al (2012) The dUTPase enzyme is essential in *Mycobacterium smegmatis*. *PLoS ONE* 7:e37461
  32. Whittingham JL, Leal I, Nguyen C et al (2005) dUTPase as a platform for antimalarial drug design: structural basis for the selectivity of a class of nucleoside inhibitors. *Structure* 13: 329–338
  33. Tormo-Más MÁ, Mir-Sanchis I, Shrestha A et al (2010) Moonlighting bacteriophage proteins derepress staphylococcal pathogenicity islands. *Nature* 465:779–782
  34. Szabó JE, Németh V, Papp-Kádár V et al (2014) Highly potent dUTPase inhibition by a bacterial repressor protein reveals a novel mechanism for gene expression control. *Nucleic Acids Res* 42:11912–11920
  35. Takács E, Grolmusz VK, Vértessy BG (2004) A tradeoff between protein stability and conformational mobility in homotrimeric dUTPases. *FEBS Lett* 566:48–54
  36. Vértessy BG, Zalud P, Nyman PO, Zeppenauer M (1994) Identification of tyrosine as a functional residue in the active site of *Escherichia coli* dUTPase. *Biochim Biophys Acta* 1205:146–150
  37. Pecsí I, Leveles I, Harmat V et al (2010) Aromatic stacking between nucleobase and enzyme promotes phosphate ester hydrolysis in dUTPase. *Nucleic Acids Res* 38:7179–7186
  38. Leveles I, Róna G, Zagyva I et al (2011) Crystallization and preliminary crystallographic analysis of dUTPase from the  $\phi$ 11 helper phage of *Staphylococcus aureus*. *Acta Crystallogr Sect F* 67:1411–1413
  39. Varga B, Migliardo F, Takacs E et al (2008) Experimental study on dUTPase-inhibitor candidate and dUTPase/disaccharide mixtures by PCS and ENS. *J Mol Struct* 886:128–135
  40. Varga B, Barabás O, Takács E et al (2008) Active site of mycobacterial dUTPase: structural characteristics and a built-in sensor. *Biochem Biophys Res Commun* 373:8–13
  41. Orosz F, Kovács J, Löw P et al (1997) Interaction of a new bis-indol derivative, KAR-2 with tubulin and its antimetabolic activity. *Br J Pharmacol* 121:947–954
  42. Hirmondó R, Szabó JE, Nyíri K et al (2015) Cross-species inhibition of dUTPase via the *Staphylococcal* StI protein perturbs dNTP pool and colony formation in *Mycobacterium*. *DNA Repair (Amst)* 30:21–27
  43. Mir-Sanchis I, Martínez-Rubio R, Martí M et al (2012) Control of *Staphylococcus aureus* pathogenicity island excision. *Mol Microbiol* 85:833–845